

Crystal Structure and Ferromagnetic Component in Layered Perovskite $\text{Sr}_{0.8}\text{Y}_{0.2}\text{CoO}_{2.65}$

I. O. Troyanchuk^{a,†}, M. V. Bushinsky^{a,*}, N. V. Tereshko^{a,**}, V. V. Sikolenko^b, and C. Ritter^c

^a Scientific–Practical Materials Research Centre, National Academy of Sciences of Belarus, Minsk, 220072 Belarus

^b Joint Institute for Nuclear Research, Dubna, Moscow oblast, 141980 Russia

^c Institut Laue–Langevin, 38042 Grenoble Cedex 9 France

*e-mail: bushinsky@physics.by

**e-mail: tereshko@physics.by

Received August 8, 2018; revised November 13, 2018; accepted November 21, 2018

Abstract—The crystal structure and magnetic state of $\text{Sr}_{0.8}\text{Y}_{0.2}\text{CoO}_{2.65}$ layered perovskite have been studied using neutron diffraction and synchrotron radiation diffraction and measuring the magnetization. It is shown that the crystal structure in the temperature range of 90–375 K can be described within the framework of the monoclinic sp. gr. $A2/m$ with a cell $4\sqrt{2}a_p \times 2\sqrt{2}a_p \times 4a_p$. The unit-cell parameter a is doubled (sp. gr. $A2/m$) below $T_N \approx 375$ K. The basic magnetic structure can be described as G -type antiferromagnetic ordering with cobalt ion magnetic moments of $2.7 \mu_B$ and $1.7 \mu_B$ in the anion-deficient $\text{CoO}_{4+\gamma}$ and stoichiometric CoO_6 layers, respectively. Based on the magnetization measurements, the ferromagnetic component of cobalt ion magnetic moment amounts to $0.27 \mu_B$ at 8 K. In both layers, the Co^{3+} ions are predominantly in the mixed low/high-spin state. The ferromagnetic component is assumed to be due to the orbital ordering in the CoO_5 pyramids at T_N and the ferromagnetic exchange coupling between CoO_5 pyramids in anion-deficient layers.

DOI: 10.1134/S1063774519060245

INTRODUCTION

Rare earth cobaltites with a perovskite structure are of great interest both from the viewpoint of technological applications and for basic research in the field of physics of magnetic phenomena [1, 2]. The state of the basic compound LaCoO_3 at low temperatures ($T \leq 30$ K) is very close to diamagnetic, whereas at temperatures above 30 K a partial spin crossover occurs from the low-spin state to the high-spin paramagnetic state [3, 4]. Doping of LaCoO_3 with Sr^{2+} up to 18% results in an occurrence of long-range ferromagnetic order [5]. At further replacement, there is an almost linear increase in the Curie temperature T_C from 180 to ~ 305 K and in the magnetization up to $M_s = 2.5 \mu_B$ for the stoichiometric compound $\text{SrCo}^{4+}\text{O}_3$, which can be obtained only under high pressure [6]. A deviation from the stoichiometric oxygen content in cobaltites gives rise to antiferromagnetic ordering, for which the Néel point may be much higher than room temperature [7]. It was shown in [8, 9] that light doping with yttrium leads to stabilization of $\text{Sr}_{1-x}\text{Y}_x\text{CoO}_{3-\delta}$ with a perovskite-type layered structure due to the large deviation from oxygen content. The CoO_6 stoichiometric layers alternate with anion-deficient $\text{CoO}_{4+\gamma}$ layers [9, 10]. The basic antiferromagnetic ordering of the G -type occurs at a point much higher than room

temperature and is accompanied by the occurrence of a small ferromagnetic component of cobalt ion magnetic moment.

A great number of scenarios of the ferromagnetic component occurrence was proposed: orbital ordering in the CoO_6 layers stoichiometric with respect to oxygen [11], uncompensated ferrimagnetic moment in anion-deficient layers [12], zigzag-like chains in stoichiometric CoO_6 layers [12], spin “bags” in these layers [13], and non-collinear magnetic structure [14]. The following questions remain open: whether the magnetic ordering is accompanied by a structural transition and what is its role in the occurrence of ferromagnetic component? To answer them, we performed a complex study of the crystal structure and magnetic and elastic properties of $\text{Sr}_{0.8}\text{Y}_{0.2}\text{CoO}_{2.65}$ and some compounds with a close yttrium content.

EXPERIMENTAL

A polycrystalline $\text{Sr}_{0.8}\text{Y}_{0.2}\text{CoO}_{2.65}$ sample was obtained by conventional ceramic technology in air. The starting reagents Y_2O_3 , Co_3O_4 , and SrCO_3 of high purity were taken in the stoichiometric ratio and carefully mixed in a Retsch PM-100 planetary ball mill with a speed of 250 rpm for 30 min. Before weighing, the Y_2O_3 oxide was preliminary annealed at a temperature of 1000°C to eliminate moisture. The sample syn-

[†] Deceased.

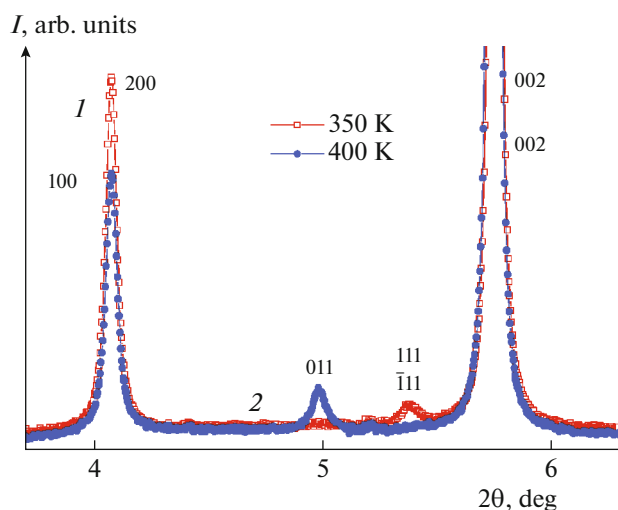


Fig. 1. (Color online) Diffraction patterns of $\text{Sr}_{0.8}\text{Y}_{0.2}\text{CoO}_{2.65}$ at (1) 350 and (2) 400 K. Indices 200, 111, $\bar{1}11$, and 002 are for the sp. gr. $A2/m$ with a superstructure $4\sqrt{2}a_p \times 2\sqrt{2}a_p \times 4a_p$; the indices 100, 011, and 002 are for the sp. gr. $A2/m$ with a superstructure $\sqrt{2}a_p \times 2\sqrt{2}a_p \times 4a_p$.

thesis involved two stages. The first was firing at 1000°C. The final synthesis was performed at 1185°C for 8 h. Then the sample was cooled to 300°C for 12 h. The oxygen content was determined with an error of ± 0.03 by the mass loss upon sample decomposition to simple oxides and metallic cobalt, as well as from the neutron diffraction data. An X-ray diffraction analysis ($T = 95\text{--}420$ K) was performed on the synchrotron radiation source at the Research Center of Paul Scherrer institute (Willingen, Switzerland). Neutron diffraction studies in the range of 10–400 K were carried out on a D2B high-resolution diffractometer at the Institut Laue–Langevin (Grenoble, France). The parameters of crystal and magnetic structures were refined by the Rietveld technique using the FullProf software package [15]. Young's modulus was measured by the method of resonance oscillations in the frequency range of 1–10 kHz. The magnetic and magnetotransport properties were investigated using a Cryogenic Ltd. setup in a magnetic field up to 14 T in the temperature range of 5–315 K. The conductivity was measured by the four-contact method; indium contacts were deposited by ultrasound.

RESULTS AND DISCUSSION

The parameters of $\text{Sr}_{0.8}\text{Y}_{0.2}\text{CoO}_{2.65}$ crystal structure were refined (using synchrotron radiation diffraction) in the space groups $I4/mmm$, $Cmma$, and $A2/m$. We could index the X-ray diffraction reflections only in the monoclinic sp. gr. $A2/m$ with the super-cell $2\sqrt{2}a_p \times 2\sqrt{2}a_p \times 4a_p$ (400 K) and $4\sqrt{2}a_p \times 2\sqrt{2}a_p \times 4a_p$ (350 K), where a_p is the primitive-cell parameter. Figure 1 shows the low-angle parts of diffraction patterns

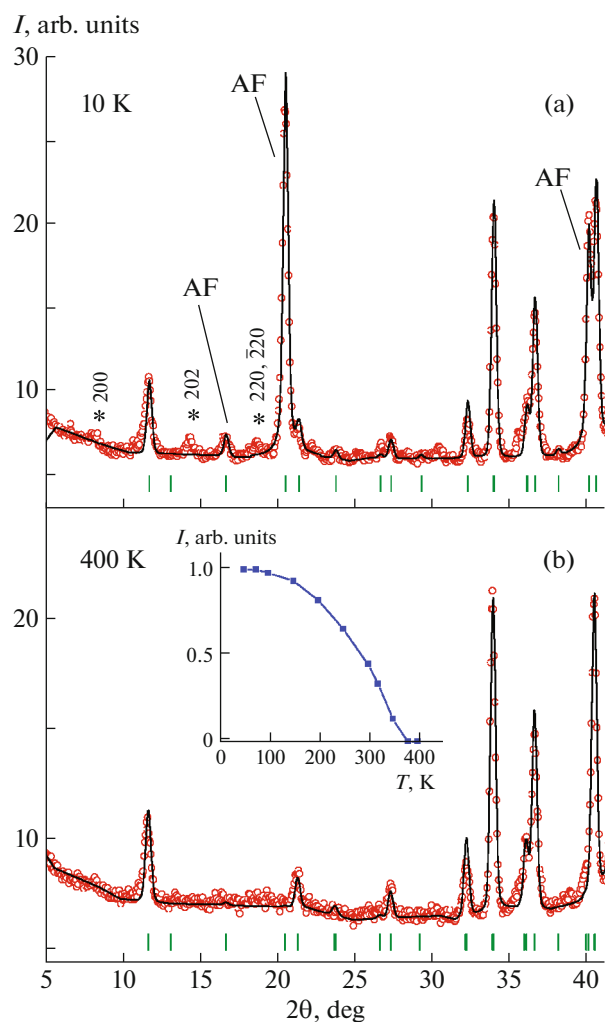


Fig. 2. (Color online) Neutron diffraction patterns of $\text{Sr}_{0.8}\text{Y}_{0.2}\text{CoO}_{2.65}$, recorded at (a) 10 and (b) 400 K. Bars indicate the Bragg reflections corresponding to the sp. gr. $I4/mmm$. Asterisks indicate the peaks that cannot be identified within the sp. gr. $I4/mmm$. The inset shows the temperature dependence of the intensity of magnetic contribution to the peak 112.

at 400 and 350 K. Changes in the diffraction peaks indicate that a phase transformation with unit-cell doubling along the a axis occurs at a temperature lying between 400 and 350 K. The unit-cell parameters are $a = 21.704$ Å, $b = 10.667$ Å, $c = 15.343$ Å, and $\gamma = 90.61^\circ$ at 10 K; $a = 21.723$ Å, $b = 10.651$ Å, $c = 15.358$ Å, and $\gamma = 90.57^\circ$ at 300 K; and $a = 10.829$ Å, $b = 10.821$ Å, $c = 15.378$ Å, and $\gamma = 90.17^\circ$ at 400 K.

Figure 2 shows the low-angle parts of neutron diffraction patterns measured at 10 and 400 K. No magnetic contribution to neutron scattering was observed at 400 K. A number of additional peaks appeared with a decrease in temperature; a part of them can be identified in the sp. gr. $I4/mmm$. These peaks are indicated by arrows and designated as AF. Very weak reflections, which can be indexed in sp. gr. $Cmma$ or $A2/m$, are indicated by asterisks. The crystal and magnetic struc-

Table 1. Ion coordinates and magnetic moments of $\text{Sr}_{0.8}\text{Y}_{0.2}\text{CoO}_{2.65}$ refined by the Rietveld technique with the sp. gr. $I4/mmm$

T , K	10	400
a, c , Å	7.6550, 15.3030	7.6603, 15.3812
V , Å ³	986.751	902.585
Sr1/Y1	0, 0, z	
Z	0.85225	0.85321
Sr2/Y2	0, 0.5, z	
z	0.86922	0.86923
Sr3/Y3	0, 0, z	
z	0.37780	0.37709
Co1	$x, y, 0$	
x	0.24873	0.25067
y	0.24873	0.25067
Co2	0.25, 0.75, 0.25	
O1	0, y, z	
y	0.24604	0.24589
z	0.25937	0.25789
O2	x, y, z	
x, y	0.21809	0.21955
z	0.11684	0.11694
O3	0, $y, 0$	
y	0.87980	0.87896
O4	$x, 0.5, 0$	
x	0.22625	0.22125
R_p/R_{wp} , %	5.13/6.61	4.51/5.97
R_{Bragg} , %	8.15	11.5
Magnetic R factor	10.2	
χ^2	13.1	10.3
Magnetic moments in CoO_6 layers, μ_B	± 1.7	
Magnetic moments in $\text{CoO}_{4+\gamma}$ layers, μ_B	± 2.7	

tures were calculated within the framework of the most simple tetragonal group $I4/mmm$ ($2a_p \times 2a_p \times 4a_p$), since the peaks that are not indexed in $I4/mmm$ are very weak. According to the Rietveld refinement, the magnetic structure of $\text{Sr}_{0.8}\text{Y}_{0.2}\text{CoO}_{2.65}$ is G -type antiferromagnetic, with magnetic moments of $1.7 \mu_B$ in the stoichiometric CoO_6 layers and $2.7 \mu_B$ in the anion-deficient ones (Table 1). The inset in Fig. 2 shows the temperature dependence of the intensity of reflection 112, from which we can see that the Néel point is about 375 K. Judging from the fact that the intensity of the reflections indicated by asterisks is greatly affected by temperature, the magnetic cell is much larger than that considered in Table 1. However, the intensity of these reflections is very low. Thus, the presented approxi-

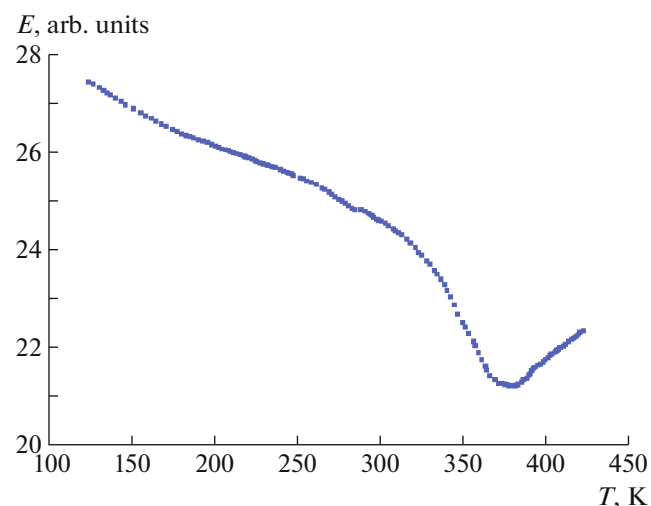
mation describes the magnetic structure rather well. According to the refined oxygen content, the cobalt ions are in the trivalent state, and the chemical formula is $\text{Sr}_{0.8}\text{Y}_{0.2}\text{CoO}_{2.65}$.

It can be seen in Fig. 3 that the Young's modulus minimum corresponds to the Néel point. This circumstance suggests that the crystal structural transformation coincides with the magnetic ordering.

It is difficult to estimate correctly the spontaneous magnetization from the field dependence of magnetization at 8 K (Fig. 4, inset) because of the absence of magnetization saturation in the fields up to 14 T. However, we can conclude that spontaneous magnetization is not lower than $0.27 \mu_B$. Generally, the temperature dependence of the magnetization has a standard shape; however an inflection is clearly seen at 280 K. Note that the compound with $x = 0.2$ has a highest spontaneous magnetization in the series $\text{Sr}_{1-x}\text{Y}_x\text{CoO}_{3-\delta}$. The temperature dependence of resistivity for the $\text{Sr}_{0.8}\text{Y}_{0.2}\text{CoO}_{2.65}$ composition exhibits semiconductor behavior; at 5 K, the resistivity amounts to $10^4 \Omega \text{ cm}$. The magnetoresistance is small and amounts to $\sim 2\%$ at 5 K in a field of 14 T.

To explain the magnetic properties, one must know the spin state of cobalt ions. Let us assume that Co^{3+} ions in both layers are in the mixed low/high-spin state. This assumption was based on the following facts.

The magnetic structure is G -type antiferromagnetic; i.e., the magnetic moments of the nearest neighbors are directed oppositely in both layers; the Néel point is high and amounts to $T_N \approx 400$ K. For the Co^{3+} ions in the intermediate spin state, the ferromagnetic interaction results in a low Curie temperature T_C . For example, $T_C \approx 90$ K in ferromagnetic epitaxial films

**Fig. 3.** (Color online) Temperature dependences of Young's modulus of $\text{Sr}_{0.8}\text{Y}_{0.2}\text{CoO}_{2.65}$.

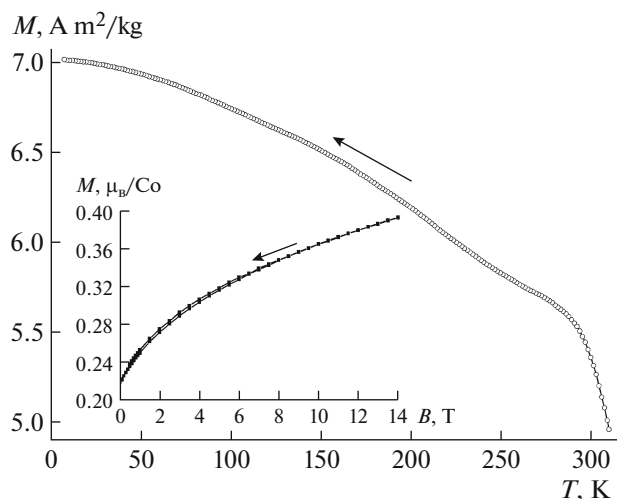


Fig. 4. Temperature dependence of the $\text{Sr}_{0.8}\text{Y}_{0.2}\text{CoO}_{2.65}$ magnetization in a magnetic field of 1 T. The inset shows the field dependence of the $\text{Sr}_{0.8}\text{Y}_{0.2}\text{CoO}_{2.65}$ magnetization at 8 K.

LaCoO_3 [16], whereas T_N amounts to 540 K for $\text{SrCoO}_{2.5}$, where cobalt ions are in the high-spin state [7]. High resistivity at 5 K ($10^4 \Omega \text{ cm}$) and low magnetoresistance indicate a good stability of the semiconductor antiferromagnetic state. The intermediate spin state is characterized by low resistivity and ferromagnetic exchange coupling.

In the CoO_6 octahedra, the Co^{3+} ion (high-spin state) is isotropic. However, if CoO_5 pyramids are connected by bases, a dedicated axis appears. It is believed that such linking of pyramids in the $\text{YBaCo}_2^{3+}\text{O}_{5.5}$ -type layered perovskites leads to a non-collinear magnetic structure and appearance of a ferromagnetic component of cobalt ion magnetic moment, which has the same value ($0.25 \mu_B$) in compounds of both classes [17, 18]. The non-collinear magnetic structure is stabilized due to the ferromagnetic bonds between cobalt ions in CoO_5 pyramids. A small substitution of iron for cobalt ions in $\text{Sr}_{0.78}\text{Y}_{0.22}\text{CoO}_{2.65}$ destroys the orbital ordering and, simultaneously, the ferromagnetic component [9].

CONCLUSIONS

It was shown that the crystal structure of layered cobaltite $\text{Sr}_{0.8}\text{Y}_{0.2}\text{CoO}_{2.65}$ can be described within the monoclinic sp. gr. $A2/m$ with a cell $2\sqrt{2}a_p \times 2\sqrt{2}a_p \times 4a_p$ at temperatures above $T_N = 375 \text{ K}$ and a cell $4\sqrt{2}a_p \times 2\sqrt{2}a_p \times 4a_p$ at temperatures below 375 K. All Co^{3+} ions are in the mixed low/high-spin state. At the temperature T_N , the unit cell increases due to the orbital ordering in the CoO_5 pyramids articulated by vertices in the anion-deficient layers. The main magnetic

structure is G -type antiferromagnetic, with a minor ferromagnetic component of the cobalt ion magnetic moment of about $0.27 \mu_B$ due to the presence of ferromagnetic exchange coupling and orbital ordering in the anion-deficient layers. The stability of the non-collinear magnetic structure is also due to the high magnetic anisotropy. The magnetic moments of the Co ions in $\text{CoO}_{4+\gamma}$ and CoO_6 layers are $2.7 \mu_B$ and $1.7 \mu_B$, respectively.

FUNDING

This study was supported by the Belarusian Republican Foundation for Fundamental Research, project no. F18R-159.

REFERENCES

1. N. B. Ivanova, S. G. Ovchinnikov, M. M. Korshunov, et al., *Usp. Fiz. Nauk* **179**, 837 (2009).
2. B. Raveau and M. M. Seikh, *Cobalt Oxides: From Crystal Chemistry to Physics* (Wiley-VCH Verlag GmbH and Co. KGaA, Weinheim, 2012).
3. A. Podlesnyak, S. Streule, J. Mesot, et al., *Phys. Rev. Lett.* **97**, 247208 (2006).
4. M. W. Haverkort, Z. Hu, J. C. Cezar, et al., *Phys. Rev. Lett.* **97**, 176405 (2006).
5. J. Wu and C. Leighton, *Phys. Rev. B* **67**, 174408 (2003).
6. Y. Long, Y. Kaneko, Sh. Ishiwata, et al., *J. Phys.: Condens. Matter* **23**, 245601 (2011).
7. A. Muñoz, C. de la Calle, J. A. Alonso, et al., *Phys. Rev. B* **78**, 054404 (2008).
8. M. James, D. Cassidy, K. F. Wilson, et al., *Solid State Sci.* **6**, 655 (2004).
9. I. O. Troyanchuk, D. V. Karpinskii, V. M. Dobryanskii, et al., *J. Exp. Theor. Phys.* **108**, 428 (2009).
10. D. V. Sheptyakov, V. Yu. Pomjakushin, O. A. Drozhzhin, et al., *Phys. Rev. B* **80**, 024409 (2009).
11. H. Nakao, T. Murata, D. Bizen, et al., *J. Phys. Soc. Jpn.* **80**, 023711 (2011).
12. D. D. Khalyavin, L. C. Chapon, E. Suard, et al., *Phys. Rev. B* **83**, 140403 (2011).
13. J. L. Bettis, H. Xiang, and M.-H. Whangbo, *Chem. Mater.* **24**, 3117 (2012).
14. I. O. Troyanchuk, M. V. Bushinskii, V. M. Dobryanskii, et al., *Pis'ma Zh. Eksp. Teor. Fiz. JETP Lett.* **94**, 849 (2011).
15. T. Roisnel and J. Rodríguez-Carvajal, *Mater. Sci. Forum.* **378–381**, 118 (2001).
16. K. Gupta and P. Mahadevan, *Phys. Rev. B* **79**, 020406 (2009).
17. M. Itoh, Y. Nawata, T. Kiyama, et al., *Physica B: Condens. Matter* **329–333**, 751 (2003).
18. J. Padilla-Pantoja, C. Frontera, O. Castaño, et al., *Phys. Rev. B* **81**, 132405 (2010).

Translated by A. Zolot'ko